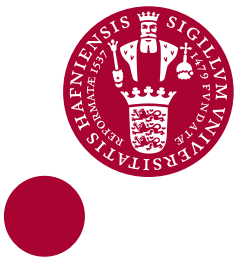

Senescence and quiescence in adipose-derived stromal cells

Effects of human platelet lysate, fetal bovine serum and hypoxia

Søndergaard, Rebekka Harary; Follin, Bjarke; Lund, Lisbeth Drozd; Juhl, Morten; Ekblond, Annette; Kastrup, Jens; Haack-Sørensen, Mandana

Published in:
Cytotherapy

DOI:
10.1016/j.jcyt.2016.09.006

Publication date:
2017

Document version
Publisher's PDF, also known as Version of record

Cytotherapy, 2017; 19: 95–106

International Society for Cellular Therapy
ISCT®

CrossMark

ADIPOSE-DERIVED STROMAL CELLS

Senescence and quiescence in adipose-derived stromal cells: Effects of human platelet lysate, fetal bovine serum and hypoxia

REBEKKA HARARY SØNDERGAARD, BJARKE FOLLIN, LISBETH DROZD LUND, MORTEN JUHL, ANNETTE EKBLOND, JENS KASTRUP & MANDANA HAACK-SØRENSEN

Cardiology Stem Cell Centre, The Heart Centre, Rigshospitalet, Copenhagen University Hospital, Copenhagen, Denmark

Abstract

Background aims. Adipose-derived stromal cells (ASCs) are attractive sources for cell-based therapies. The hypoxic niche of ASCs *in vivo* implies that cells will benefit from hypoxia during *in vitro* expansion. Human platelet lysate (hPL) enhances ASC proliferation rates, compared with fetal bovine serum (FBS) at normoxia. However, the low proliferation rates of FBS-expanded ASCs could be signs of senescence or quiescence. We aimed to determine the effects of hypoxia and hPL on the expansion of ASCs and whether FBS-expanded ASCs are senescent or quiescent. *Methods.* ASCs expanded in FBS or hPL at normoxia or hypoxia until passage 7 (P7), or in FBS until P5 followed by culture in hPL until P7, were evaluated by proliferation rates, cell cycle analyses, gene expression and β-galactosidase activity. *Results.* hPL at normoxia and hypoxia enhanced proliferation rates and expression of cyclins, and decreased G0/G1 fractions and expression of p21 and p27, compared with FBS. The shift from FBS to hPL enhanced cyclin levels, decreased p21 and p27 levels and tended to decrease G0/G1 fractions. *Conclusion.* Hypoxia does not add to the effect of hPL during ASC expansion with regard to proliferation, cell cycle regulation and expression of cyclins, p21 and p27. hPL rejuvenates FBS-expanded ASCs with regard to cell cycle regulation and expression of cyclins, p21 and p27. This indicates a reversible arrest. Therefore, we conclude that ASCs expanded until P7 are not senescent regardless of culture conditions.

Key Words: *adipose-derived stromal cells, clinical therapy, fetal bovine serum, human platelet lysate, hypoxia, quiescence, senescence*

Introduction

Over the years, adipose-derived stromal cells (ASCs) have gained increasing attention because of their relatively high abundance, easier accessibility and higher proliferation rates *in vitro*, compared with mesenchymal stromal cells from bone marrow (BMSCs) [1].

ASCs reside in a hypoxic niche *in vivo*, which suggests that hypoxic conditions during *in vitro* expansion might be beneficial [2]. Indeed, hypoxia has been shown to enhance *in vitro* proliferation rates of ASCs cultured in fetal bovine serum (FBS) [3–5]. Human platelet lysate (hPL) enhances ASC proliferation rates, compared with FBS. Thus, a combination of hypoxia and hPL might enhance ASC proliferation rates and prevent senescence during culture expansion [2,4–6]. However, the low proliferation rates of ASCs expanded in FBS at normoxia could potentially be due to the presence of quiescent or slowly proliferating cells, rather than senescent cells.

Regulation of ASC proliferation is mediated by cyclins, which drive progression through the cell cycle. Of these, cyclin E has been shown to be essential and rate-limiting for transition through the first checkpoint, known as G1/S [7,8]. Quiescent and slowly proliferating cells share a number of common features including large proportions of cells in G0/G1 phase, high expression levels of p21 and p27, and reversibility. This means that quiescent and slowly proliferating cells will reinitiate or increase proliferation and decrease the proportions of cells in G0/G1

Correspondence: **Mandana Haack-Sørensen**, PhD, Cardiology Stem Cell Centre, The Heart Centre, Rigshospitalet, Copenhagen University Hospital, DK-2100 Copenhagen Ø, Denmark. E-mail: Mandana.haack-soerensen@regionh.dk

(Received 7 March 2016; accepted 9 September 2016)

http://dx.doi.org/10.1016/j.jcyt.2016.09.006

phase in response to mitogenic stimulation [9,10]. In the case of quiescent cells, reversibility is dependent on transcription factor HES1, which suppresses senescence and terminal differentiation [11].

In contrast to the reversible cell states, the cell cycle arrest of senescence is essentially irreversible. Once senescent, cells will not re-enter the cell cycle if the senescence-inducing stimuli are terminated [12], nor will senescent cells respond to mitogenic stimulation [13]. The features of senescent cells include high expression levels of p21 and $p16^{INK4A}$, and increased senescence-associated β-galactosidase activity [9,14,15].

Because senescent cells acquire functional abnormalities, their presence in a clinical cell product could compromise efficacy [16,17]. Therefore, we have, with modifications, adapted the excellent study design of Griffiths *et al.* to distinguish reversible cell states from irreversible senescence in our FBS cultures [18]. Griffiths *et al.* demonstrated that hPL completely rejuvenates middle passage (P6–P8) BMSCs expanded in FBS, whereas late passage (P15-16) BMSCs only respond transiently to a shift to hPL before their proliferation is significantly impaired [18]. This suggests that BMSCs P6–P8 are reversibly arrested, while BMSCs P15–16 are irreversibly arrested, and hence senescent.

At our stem cell centre, FBS-expanded ASCs and BMSCs used for clinical trials do not exceed P3 [19–22]. We have chosen to expand ASCs cultured in FBS for two additional passages (until P5) before subjecting them to our test for reversibility. In addition, we have included the combination of hypoxia and clinically approved hPL to determine the optimal culture conditions for clinical ASC production.

The aim of this study was to investigate whether our ASC cell product is devoid of senescent cells, regardless of the media supplements FBS and hPL and oxygen tension. This was investigated based on proliferation rates, cell cycle analysis, gene expression and senescence-associated β-galactosidase activity.

Methods

Experimental design

ASCs isolated from the stromal vascular fraction (SVF) of adipose tissue were cultured in two clinically approved complete media containing either hPL or FBS, at normoxic or hypoxic (5% O_2) conditions. ASCs were expanded until P7 at the following conditions: (i) FBS, (ii) FBS hypoxia, (iii) hPL, (iv) hPL hypoxia, (v) P5 FBS shifted to hPL and (vi) P5 FBS hypoxia shifted to hPL hypoxia (Figure 1).

To avoid contact inhibition-induced quiescence, cell cycle analysis was performed and RNA was extracted from a pool of sub-confluent ASCs.

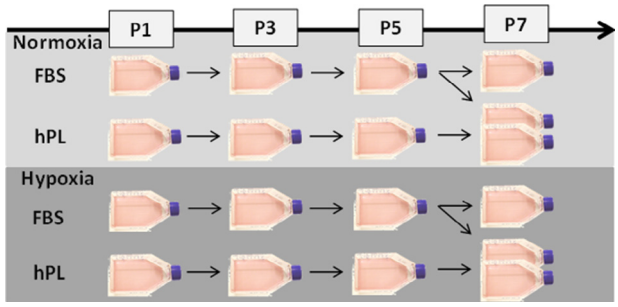

Figure 1. Flow chart of the experimental design.

Lipoaspirate preparation and SVF isolation

Lipoaspirate was obtained from three healthy donors (one male, two females, aged 23–55 years, mean age 35 years). The use of lipoaspirate from healthy volunteers was approved by the National Ethical Committee protocol no. H-3-2009-119. All donors agreed to and signed the informed written consent.

Approximately 100 mL lipoaspirate was obtained from liposuction of subcutaneous abdominal fat performed under local anaesthesia. The lipoaspirate was washed 2–4 times with phosphate buffered saline (PBS) pH 7.4 (Gibco, Life Technologies) to remove residual blood. The adipose tissue was digested by incubation with 0.6 PZ U/mL collagenase NB 4 (Serva) dissolved in HBSS (2 mmol/L Ca^{2+}, Life Technologies) at 37°C for 45–55 min, at constant rotation. The collagenase was inactivated with complete medium containing 10% FBS (Irradiated, Gibco, Life Technologies), followed by filtration through a 100-µm mesh (Steriflip Filtration System, Millipore). Cells were centrifuged for 10 min at 1200*g*, resuspended in complete medium containing FBS or hPL and cell number and viability were measured using NucleoCounter NC-100 (Chemometec) according to manufacturer's instructions.

Cell culture

SVF cells were seeded in T-75 flasks (Thermo Fisher Scientific) at a density of 4.5×10^6 cells/flask in complete medium containing Minimum Essential Medium alpha (αMEM) (Gibco, Life Technologies) with 1% penicillin/streptomycin (Gibco, Life Technologies) and one of the following supplements: 10% FBS or 5% hPL (Stemulate, Cook Regentec). The FBS batch has previously been used in our clinical studies [19–22], and thus it has been pre-qualified for ASC culture.

SVF cells were incubated at normoxic conditions (37°C, 5% CO_2, 21% O_2, humidified air). On the third day of culture, cells were washed twice with PBS to remove non-adherent cells. Subsequently, medium was changed every 3–4 days.

ASCs P1 and subsequent passages were cultured at either normoxic or hypoxic (37°C, 5% CO_2, 5% O_2, humidified air) conditions.

Upon reaching ≥80% confluence, cells were harvested by incubation with 3 mL TrypLE Select (Gibco, Life Technologies) for 10 min, at normoxic conditions. TrypLE was inactivated with 7 mL complete medium containing FBS or hPL, and cells were counted and re-seeded at a density of 3.5×10^5 cells/T-75 flask in 15 mL complete medium containing FBS or hPL.

Proliferation

Population doublings (PDs) were calculated from P1 using the formula: PD = (log N—log N_0)/log 2, where N is the number of harvested cells and N_0 is the number of seeded cells. Cumulative population doublings (cPDs) were defined as the sum of all successive PDs.

Phenotypic characterization

Cells were characterized according to the guidelines established by the International Society for Cellular Therapy (ISCT) and the International Federation for Adipose Therapeutics and Science (IFATS) at the end of P1 [23,24]. Cells were washed in flow cytometry PBS containing fluorescence activated cell sorting (FACS) PBS (Hospital Pharmacy), 1% ethylenediaminetetraacetic acid (EDTA) (Hospital Pharmacy) and 10% newborn calf serum (Gibco, Life Technologies) and incubated with antibodies (1.5×10^5 cells per sample) for 30 min at room temperature, protected from light. The antibodies were as follows: CD105-phycoerythrin (PE) (clone 166707, R&D Systems), CD90-fluorescein isothiocyanate (FITC) (F15-42-1-5), CD13-phycoerythrin-Texas Red (ECD) (Immu103.44), CD34-allophycocyanin (APC) (581), HLA-DR-FITC (B8.12.2), CD19-ECD (J3-119), CD14-PE-Cyanin 7 (PECy7) (RMO52), CD29-FITC (K20) (all from Beckman Coulter), and CD73-PE (AD2), CD45-FITC (2D1), CD31-FITC (WM59), CD36-FITC (CB38), CD106-FITC (51-10C9), CD166-PE (3A6) all from BD Biosciences. After incubation, cells were washed in flow cytometry PBS, re-suspended in PBS and analyzed on a Navios flow cytometer (Beckman Coulter), using a fluorescence minus one protocol. Cell viability was determined by labeling with 1 µL Sytox Blue (Life Technologies) for 5 min, before analysis. At least 5000 live cells were acquired per sample. Data were analyzed with Navios software and Kaluza (Beckman Coulter), with discrimination of dead cells and doublets.

Cell cycle assay

Sub-confluent cells (5×10^5) were fixed in 70% ice-cold ethanol, added drop-wise while vortexing and incubated for 30 min, on ice. After fixation, cells were washed in ice-cold flow cytometry PBS and centrifuged for 10 min, at 800*g*. Cells were incubated with 500 µL Propidium iodide/RNase staining buffer (BD Biosciences) for 15 min at room temperature, protected from light. Following incubation, cells were washed, re-suspended in flow cytometry PBS and analyzed on a BD FACS Canto II (BD Biosciences). Ten thousand cells were acquired per sample. Data analysis was performed using FlowJo version 10 software (Treestar). Cells were gated on forward and side scatter, and cell debris was excluded. The percentage of cells in G0/G1-, S- and G2/M-phase were calculated as a function of DNA content by fitting data to the Dean-Jett-FOX model (see Supplementary Figure S1).

Quantitative polymerase chain reaction

Total RNA was extracted from sub-confluent cells using Qiagen RNeasy Mini Kit (Qiagen) according to manufacturer's protocol. RNA purity was validated using a NanoDrop 1000 Spectrophotometer (Thermo Scientific) with A260/A280 and A260/A230 minimum criteria of 1.7–2.2.

cDNA synthesis was prepared using AffinityScript (Stratagene, Agilent Technologies) according to manufacturer's protocol.

Quantitative polymerase chain reaction (qPCR) was performed using Brilliant II SYBR Green QPCR master mix with low reference dye ROX (Agilent Technologies), as described previously [25]. cDNA was diluted in Tris-EDTA buffer (Sigma-Aldrich) and subsequently in RNase-DNase-free water (5 Prime) and added to each well along with primers (Life Technologies), SYBR Green and RNase-DNase-free water, giving a total reaction volume of 25 µL/well. qPCR reactions were performed on an Mx3000 (Stratagene, AH-diagnostics), and results were collected using Mx3000 version 4.0 software for Windows (Stratagene, AH-diagnostics). The reactions were performed at 95°C for 10 min, followed by 40 cycles at 60°C for 1 min, and 95°C for 30 s. Reaction samples were performed in duplicates. "No template" and "no reverse transcriptase" controls were included for each reaction plate.

Primers were designed using the NCBI Primer-BLAST tool (as shown in Supplementary Figure S2). Primers had no predicted secondary structures of target sequences using Mfold [26] and were checked for primer-dimers using AutoDimer [27]. A standard curve was included for each qPCR reaction plate, and data were only included if the reaction efficiency fulfilled the minimum criteria of 100% ± 5 using seven or eight data points. TATA box-binding protein (TBP) and Tyrosine 3-monooxygenase/tryptophan 5-monooxygenase activation protein (YWHAZ) were selected as reference genes due to their stable expression in ASCs with

increasing passage and at hypoxia [28,29]. The fold change in gene expression of target genes is shown in relation to the geometric mean of TBP and YWHAZ (ΔCq), with $2^{\Delta Cq}$ as the fold change in expression levels. Analysis of significance was performed using $2^{\Delta Cq}$.

β-galactosidase staining

Endogenous β-galactosidase activity was detected using a β-Gal Staining Kit (Life Technologies) according to manufacturer's protocol. In 24-well plates (NUNC, Thermo Fischer Scientific), 5×10^3 cells/cm^2 were seeded in complete medium containing FBS or hPL. Preparation of solutions was performed in polystyrene-free tubes (CELLSTAR, VWR). X-Gal in N,N-dimethylformamide (Sigma-Aldrich Chemie) was freshly prepared for each staining. Cells were incubated with staining solution for 24 h at normoxic conditions. Cells were visualized by bright field microscopy using an IX51 microscope (Olympus), a DP71 digital camera (Olympus) and ImageProPlus 7.0 software (Media Cybernetics).

Statistics

All comparisons were initially performed using repeated-measures analysis of variance. When data were not dependent on passage number, subsequent analysis using paired *t*-test with Sidak correction were performed. Sidak correction resulted in the significance level being set to $P < 0.025$ for these comparisons (Figures 4, 5 and 6). Analysis using paired *t*-test without Sidak correction was performed due to fewer comparisons, resulting in the significance level being set to $P < 0.05$ (Figure 3; and Table II). All statistics were performed with SPSS (IBM). All values are expressed as mean ± SD unless otherwise stated. All data is based on ASCs from three donors (n = 3).

Results

Phenotypic characterization

The phenotypes of ASCs P1 were characterized according to the ISCT and IFATS guidelines (Table I) [23,24]. Regardless of culture conditions, ASCs expressed uniformly high levels (>90%) of stromal markers CD73, CD90, CD105, CD13, CD29 and CD166; medium levels (10–30%) of CD36; and low (2–5%) to very low levels (<2%) of CD45, CD34, HLA-DR, CD19, CD14, CD106 and CD31.

Morphology

ASCs FBS varied in cell size and shape, with a subset of cells appearing enlarged and flattened (Figure 2). ASCs FBS hypoxia contained fewer enlarged cells, compared with FBS at normoxia. ASCs cultured in hPL at normoxia and hypoxia appeared homogenous with thin, spindle-like morphologies. The morphologies of ASCs did not change with increasing passage.

Table I. Surface antigen expression of P1 ASCs cultured in FBS or hPL at normoxia or hypoxia.

	FBS	FBS hypoxia	hPL	hPL hypoxia
CD73	>90%	>90%	>90%	>90%
CD90	>90%	>90%	>90%	>90%
CD105	>90%	>90%	>90%	>90%
CD13	>90%	>90%	>90%	>90%
CD29	>90%	>90%	>90%	>90%
CD166	>90%	>90%	>90%	>90%
CD36	10–30%	10–30%	10–30%	10–30%
CD45	<2%	<2%	<2%	2–5%
CD34	2–5%	<2%	2–5%	<2%
HLA-DR	<2%	<2%	<2%	2–5%
CD19	<2%	<2%	<2%	<2%
CD14	2–5%	2–5%	<2%	<2%
CD106	<2%	<2%	<2%	<2%
CD31	<2%	<2%	<2%	2–5%

Data are the mean percentage of positive cells from three donors (n = 3), categorized into groups: > 90%, 10–30%, 2–5% and <2%.

Proliferation kinetics

ASCs expanded in FBS proliferated at low rates (13.1 ± 0.2 cPDs after seven passages) (Figure 3). Hypoxia tended to increase the proliferation rates of FBS-expanded ASCs (18.4 ± 2.6 cPDs), although not significantly ($P = 0.269$). hPL significantly increased the proliferation rates of ASCs, compared with FBS (24.5 ± 1.9 cPDs, $P = 0.014$). The proliferation rates of ASCs hPL hypoxia were also significantly increased compared with FBS (24.3 ± 1.4 cPDs, $P = 0.018$). Hypoxia had no effect on the proliferation rates of ASCs expanded in hPL ($P = 1.000$).

Cell cycle analysis

The cell cycle distributions of ASCs were investigated by flow cytometry, and the proportion of cells in G0/G1 phase was used as a measure of non-cycling cells.

A large proportion of P1 FBS and P1 FBS hypoxia cultures were in G0/G1 phase (89.1 ± 5.7% and 84.8 ± 4.7%, respectively) (Figure 4). Hypoxia had no effect on the G0/G1 fraction of P1 FBS cultures ($P = 0.336$). The G0/G1 fractions were significantly lower for P1 hPL and P1 hPL hypoxia, compared with P1 FBS (52.6 ± 8.8%, $P = 0.004$ and 52.7 ± 10.9%, $P = 0.010$, respectively).

The cell cycle distributions of ASCs FBS, hPL and hPL hypoxia were similar at P1, P3 and P5, while hypoxia tended to decrease the G0/G1 fractions of FBS-expanded ASCs at P3 and P5, compared with P1.

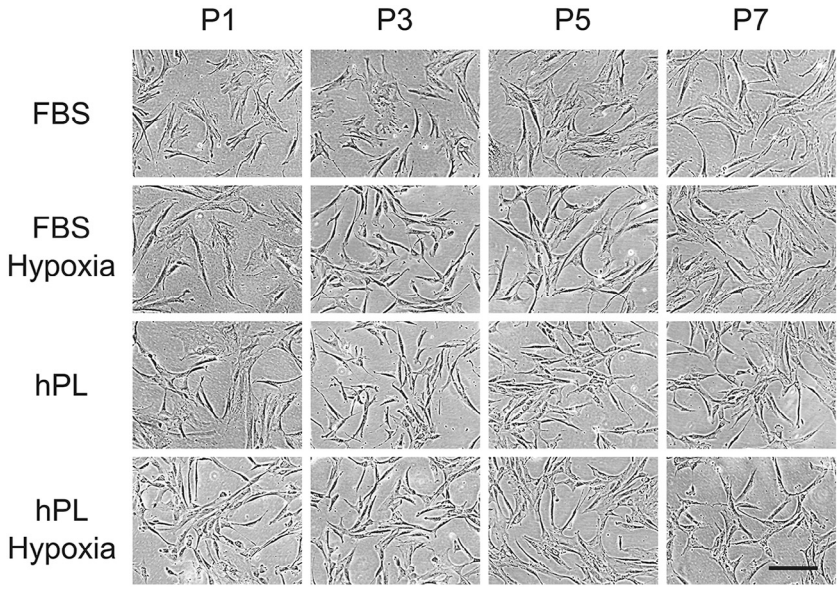

Figure 2. Morphology of ASCs expanded in FBS or hPL at normoxia or hypoxia. Scale bar: 200 μm.

At P7, the G0/G1 fractions for FBS cultures (87.7 ± 6.5%) were generally higher compared with FBS hypoxia, hPL and hPL hypoxia (74.2 ± 5.6%, 75.1 ± 12.8% and 64.3 ± 10.1%, respectively), and the difference between FBS and hPL hypoxia was significant ($P = 0.008$).

Expression of cyclins

The expression of cyclins, which regulate cell cycle progression, was measured by qPCR.

G1 phase: Overall, the expression levels of the early G1 phase cyclin D1 tended to be comparable or slightly higher in FBS and FBS hypoxia, compared with hPL and hPL hypoxia (Figure 5A). Cyclin D1 levels tended to increase with increasing passage in FBS hypoxia. However, no significant differences were found.

The late G1 phase cyclin E1 was expressed at higher levels in P1 hPL and P1 hPL hypoxia, compared with P1 FBS and P1 FBS hypoxia (Figure 5B), with the difference between hPL and FBS being significant ($P = 0.020$). Cyclin E1 levels in FBS remained low with increasing passage. In contrast, cyclin E1 levels in FBS hypoxia increased from P3 and onward, compared with P1. The relatively high expression of cyclin E1 in hPL and hPL hypoxia was maintained with increasing passage. At P7, cyclin E1 levels tended to be higher in hPL and hPL hypoxia, compared with FBS ($P = 0.060$ and $P = 0.038$, respectively).

S phase: The expression patterns of the S phase cyclin A2 were similar to the expression patterns of cyclin E1 (Figure 5C). The only exception was a relative increase in P1 FBS hypoxia, which was not seen for cyclin E1. At P1, the expression levels of cyclin A2 were significantly higher in hPL and hPL hypoxia, compared with FBS ($P = 0.008$ and $P = 0.001$, respectively). The expression levels of cyclin A2 were similar during serial passaging. At P7, cyclin A2 levels were significantly higher in hPL hypoxia, compared with FBS ($P = 0.014$).

G2/M phase: The expression patterns of the G2/M phase cyclin B1 were similar to the expression patterns of cyclin A2 (Figure 5D). The expression levels of cyclin B1 were significantly higher in P1 hPL and P1 hPL hypoxia, compared with P1 FBS ($P = 0.004$ and $P = 0.007$, respectively). At P7, cyclin B1 levels were significantly higher in hPL hypoxia compared to FBS ($P = 0.021$).

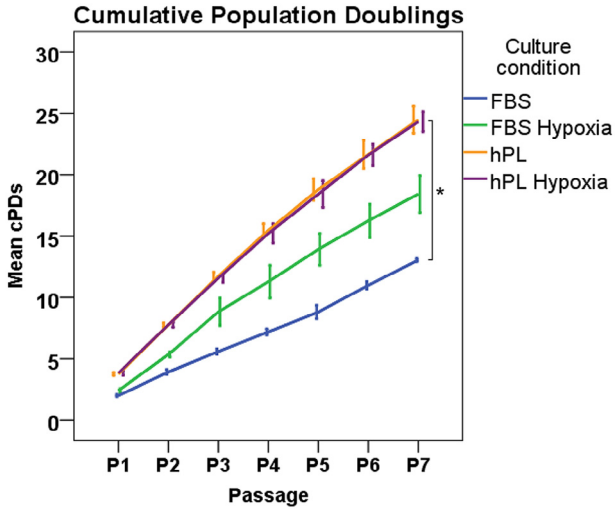

Figure 3. Proliferation curves for ASCs P1–P7 expanded in FBS or hPL at normoxia or hypoxia. Data is shown as mean cPDs ± SE, based on ASCs from three donors (n = 3). Significance level is $P < 0.05$, indicated by *.

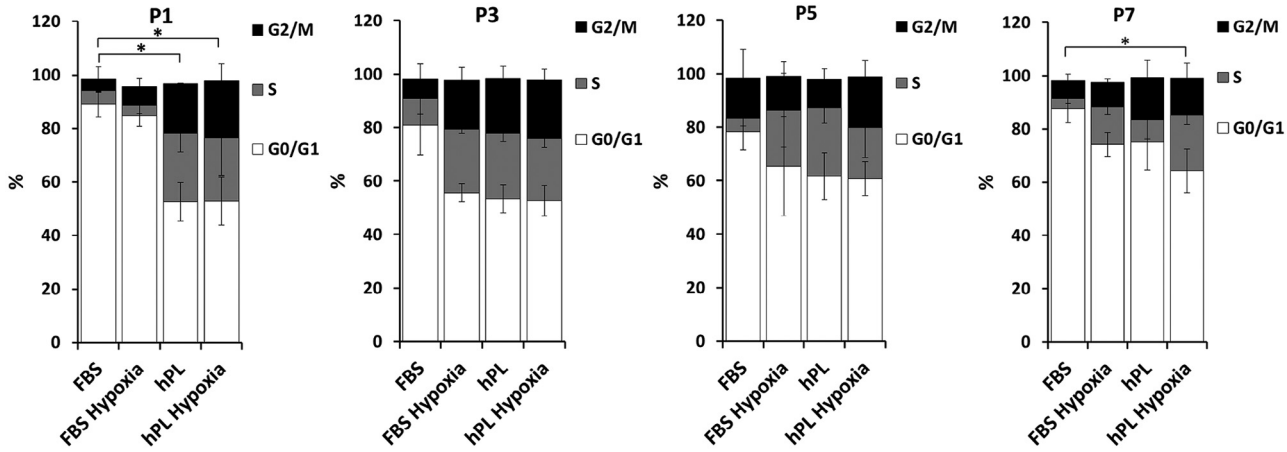

Figure 4. Cell cycle distributions of ASCs expanded in FBS or hPL at normoxia or hypoxia. Data is shown as mean percentages of cells in G0/G1, S, and G2/M phase ± SE, based on ASCs from three donors (n = 3). Significance level is $P < 0.025$, indicated by *.

Expression of senescence and quiescence markers

The expression of senescence marker $p16^{INK4A}$, senescence and quiescence marker p21 and quiescence markers p27 and HES1 was measured by qPCR.

p21: ASCs FBS expressed relatively high levels of the cell cycle inhibitor p21, and the levels of p21 did not increase with increasing passage (Figure 6A). Hypoxia tended to decrease p21 levels in FBS cultures. Culture in hPL or in hPL at hypoxia also tended to decrease p21 expression in ASCs P1, compared with ASCs P1 FBS ($P = 0.066$ and $P = 0.075$, respectively). This trend was maintained during serial-passaging. At P7, the expression of p21 was significantly lower in hPL and hPL Hypoxia, compared with FBS ($P = 0.009$ and $P = 0.014$, respectively).

p27: Generally, the expression levels of the cell cycle inhibitor p27 were higher in FBS and FBS hypoxia compared with hPL and hPL hypoxia (Figure 6B). At P5, the p27 expression levels were significantly lower in hPL, compared with FBS ($P = 0.013$).

$p16^{INK4A}$: ASCs generally expressed low levels of the senescence marker $p16^{INK4A}$ according to different culture conditions (Figure 6C). There was a small non-significant increase in $p16^{INK4A}$ expression levels in ASC FBS hypoxia at P5 and P7, compared with ASCs cultured at the other conditions. This was due to one ASC donor that generally had higher $p16^{INK4A}$ levels, and especially in FBS hypoxia at P5 and P7, compared with the two other ASC donors (Supplementary Figure S3).

HES1: The expression of quiescence marker HES1 showed great variations between ASCs from different donors (Figure 6D). Overall, HES1 expression levels tended to be higher in FBS and FBS hypoxia, compared with hPL and hPL hypoxia.

Senescence-associated β-galactosidase activity

Regardless of the media supplements FBS and hPL and oxygen tension, ASCs expanded until P7 were completely negative for senescence-associated β-galactosidase activity (data not shown).

Effects of shifting from FBS to hPL or from FBS hypoxia to hPL hypoxia

The effects of shifting ASCs from FBS to hPL or from FBS hypoxia to hPL hypoxia can be seen in Figure 7 and Table II.

Morphology: When ASCs were shifted from FBS to hPL or from FBS hypoxia to hPL hypoxia, they generally acquired the morphology of hPL-cultured cells, whereas only a small fraction of cells maintained FBS-like morphology (Figure 7).

Cell cycle analysis: The shift from FBS to hPL reduced the G0/G1 fractions of ASCs (60.5 ± 7.3%), compared to FBS (87.7 ± 6.5%, $p = 0.075$), as shown in Table II. This made the G0/G1 fraction of ASCs FBS to hPL comparable to that of ASCs hPL (75.1 ± 12.8%). The shift from FBS at hypoxia to hPL at hypoxia had no effect on G0/G1 fractions (64.1 ± 8.5%), compared with FBS hypoxia (75.1 ± 12.8%, $P = 0.204$).

Expression of cyclins: The shift from FBS to hPL significantly enhanced expression of cyclin E1 ($P = 0.004$), cyclin A2 ($P = 0.016$) and cyclin B1 ($P = 0.018$), compared with FBS, whereas cyclin D1 expression was not affected ($P = 0.374$; Table II). The expression of cyclins in ASCs FBS hypoxia to hPL hypoxia did not show significant differences compared to FBS hypoxia.

Expression of senescence and quiescence markers: Shifting ASCs from FBS to hPL significantly decreased

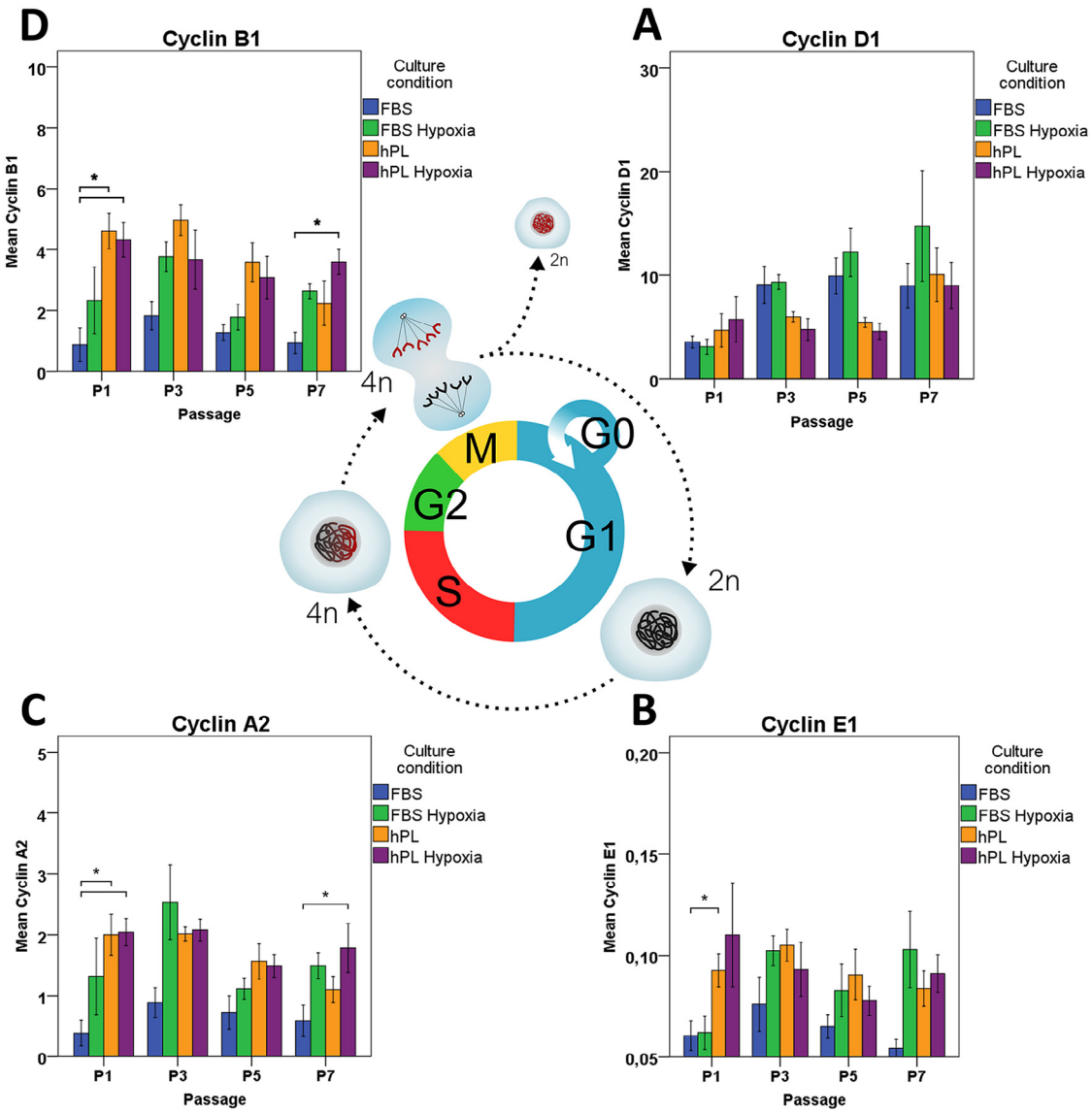

Figure 5. mRNA levels of the four cyclins in ASCs expanded in FBS or hPL at normoxia or hypoxia, and their role in the different cell cycle phases. (A) Expression of the early G1 phase cyclin D1. (B) Expression of the late G1 phase cyclin E1. (C) Expression of the S phase cyclin A2. (D) Expression of the G2 and M phase cyclin B1. Data is shown as mean expression levels (2ΔCq) ± SE, based on ASCs from three donors (n = 3). Significance level is $P < 0.025$, indicated by *.

Table II. Effects of shifting from FBS to hPL or from FBS hypoxia to hPL hypoxia on G0/G1 fractions and mRNA levels of ASCs P7.

	FBS	FBS to hPL	*P* value	FBS hypoxia	FBS hypoxia to hPL hypoxia	*P* value	Units
G0/G1	87.7 ± 6.5	60.5 ± 7.3	0.075	74.2 ± 5.6	64.1 ± 8.5	0.204	Percentage
p21	7.96 ± 1.46	1.72 ± 0.54	0.010*	4.99 ± 1.89	1.44 ± 0.24	0.333	Relative expression
p27	0.45 ± 0.13	0.27 ± 0.10	0.032*	0.49 ± 0.39	0.23 ± 0.05	0.129	Relative expression
Cyclin D1	8.97 ± 3.73	6.08 ± 0.70	0.374	14.74 ± 9.27	7.98 ± 3.44	0.201	Relative expression
Cyclin E1	0.05 ± 0.01	0.11 ± 0.01	0.004*	0.10 ± 0.03	0.09 ± 0.04	0.686	Relative expression
Cyclin A2	0.59 ± 0.45	1.58 ± 0.57	0.016*	1.49 ± 0.37	1.12 ± 0.39	0.382	Relative expression
Cyclin B1	0.93 ± 0.61	3.93 ± 1.06	0.018*	2.64 ± 0.43	3.20 ± 1.08	0.435	Relative expression

FBS to hPL data compared with FBS data. FBS hypoxia to hPL hypoxia data are compared with FBS hypoxia data. qPCR data are presented as $2^{\Delta Cq}$. All data are shown as means ± SD, based on ASCs from three donors (n = 3). *Significance level: $P < 0.05$.

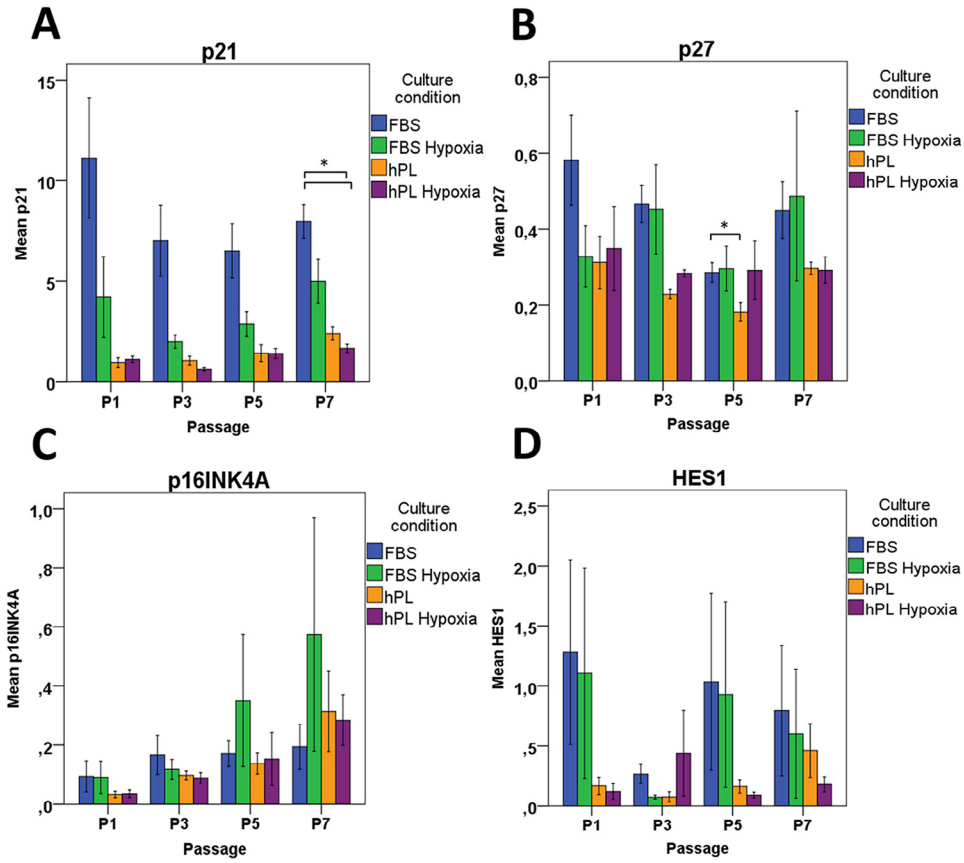

Figure 6. mRNA levels of p21, p27, $p16^{INK4A}$ and HES1 in ASCs expanded in FBS or hPL at normoxia or hypoxia. (A) Expression of senescence and quiescence marker p21. (B) Expression of quiescence marker p27. (C) Expression of senescence marker $p16^{INK4A}$. (D) Expression of quiescence marker HES1. Data is shown as mean expression levels (2ΔCq) ± SE, based on ASCs from three donors (n = 3). Significance level is $P < 0.025$, indicated by *.

expression of p21 ($P = 0.010$) and p27 ($P = 0.032$), compared with FBS (Table II). In contrast, there were no effects on expression levels of $p16^{INK4A}$ or HES1 (data not shown). The expression of senescence and quiescence markers in ASCs FBS hypoxia to hPL hypoxia did not show significant differences compared with FBS hypoxia.

β-galactosidase activity: ASCs FBS to hPL and FBS hypoxia to hPL hypoxia were completely negative for β-galactosidase activity (data not shown).

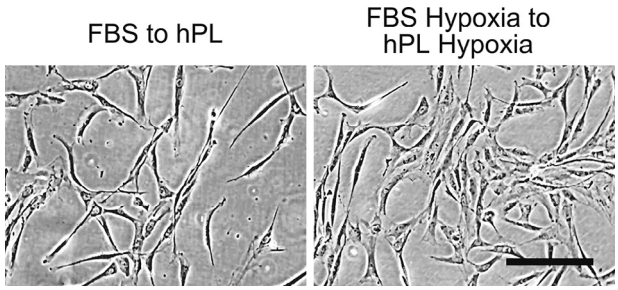

Figure 7. Morphology of ASCs P7 shifted from FBS to hPL or from FBS hypoxia to hPL hypoxia. Scale bar: 200 µm.

Discussion

This study investigated the effects of the media supplements FBS and hPL and oxygen tension on proliferation, quiescence and senescence in human ASCs expanded until P7.

Initially, ASCs P1 cultured in FBS or hPL at normoxia or hypoxia were characterized according to the ISCT and IFATS guidelines. The rationale behind characterizing ASCs P1 was that these were used as the earliest "time point"/starting point in our subsequent analyses. As expected, ASCs P1 contained some levels of non-stromal cells. However, we think it unlikely that this affected the results in our subsequent analyses. Additionally, the levels of non-stromal cells will diminish with further culture expansion [24].

We found that ASCs culture expanded in FBS proliferated at low rates, had large G0/G1 fractions and expressed low levels of cyclins E1, A2 and B1 and high levels of p21. The increasing cPDs with increasing passage shows that the ASC FBS population as a whole is proliferating, and hence not senescent or quiescent. However, it is possible that senescent or quiescent subpopulations are present.

It has been shown that BMSCs FBS enter replicative senescence at 41 ± 10 cPDs, referred to as the Hayflick limit [30]. Because BMSCs enter replicative senescence earlier than ASCs, the Hayflick limit of ASCs is likely to be higher [31]. In our study, the numbers of reached cPDs were far below the Hayflick limit, suggesting that ASCs are not replicatively senescent. The lack of expression of $p16^{INK4A}$, the cell cycle inhibitor that is especially important for ASC senescence [14,15], further supports that ASCs expanded until P7 do not contain senescent subpopulations regardless of the media supplements FBS and hPL and oxygen tension. We did find a non-significant increase in $p16^{INK4A}$ mRNA levels in FBS hypoxia cultures at P5 and P7, which was due to a relatively higher $p16^{INK4A}$ level in one ASC donor, compared with the two other ASC donors. However, because the $p16^{INK4A}$ protein stabilizes p21 mRNA [32], the lack of a corresponding increase in p21 mRNA implies that ASCs expanded until P7 do not express the $p16^{INK4A}$ protein, regardless of the culture conditions tested here. It has been shown that $p16^{INK4A}$ mRNA is significantly up-regulated in ASCs FBS at 17 cPDs [15]. However, this does not necessarily mean that the $p16^{INK4A}$ protein is up-regulated.

The final test for reversible cell states versus irreversible senescence in our FBS cultures was rejuvenation with a richer growth medium. Even though one ASC donor had a higher $p16^{INK4A}$ level compared with the two other ASC donors, ASCs from all three donors were able to respond to the mitogenic stimuli of hPL. Indeed, the shift from FBS to hPL decreased G1/G0 fractions, significantly enhanced expression of cyclins E1, A2 and B1, and significantly decreased expression of p21 and p27, compared with FBS. Therefore, our ASC product expanded in FBS until P7 is not irreversibly arrested and hence not senescent.

The ASCs used in our clinical studies are not expanded beyond P3. On the basis of our findings, we are certain that the ASC product used in our clinical studies is senescence-free.

We do not find it relevant for our clinical setting to determine the passage threshold range at which our ASC product becomes senescent. On the basis of the high inter-donor variability in $p16^{INK4A}$ expression, we predict that the process would be elaborate and time-consuming.

However, it is likely that ASC donors with higher $p16^{INK4A}$ levels would reach the senescence threshold earlier than ASC donors with low $p16^{INK4A}$ levels. Therefore, if ASCs at higher passages than P7 are used clinically, we suggest that screening ASCs from different donors for $p16^{INK4A}$ expression using qPCR could provide a useful estimate or prediction of senescence.

Griffiths *et al.* demonstrated that the shift from FBS to hPL completely rejuvenated BMSCs P6–P8, whereas BMSCs P15–16 only responded transiently to the shift to hPL, before significantly impaired proliferation was observed [18]. This suggests a senescence threshold range for BMSCs around P15–16. If BMSCs FBS become senescent and show impaired growth factor responsiveness at P15–P16, the corresponding response in ASCs would probably occur at similar or later passages because BMSCs enter replicative senescence earlier than ASCs [31].

We did not detect any senescence-associated β-galactosidase activity in ASCs expanded until P7 regardless of the medium supplements FBS and hPL and oxygen tension. This finding also suggests that ASCs do not contain senescent subpopulations. An increase in β-galactosidase activity has been demonstrated in ASCs FBS at 17 cPDs [15].

The lack of β-galactosidase activity further implies that ASCs expanded until P7 do not express $p16^{INK4A}$ because a positive correlation exists between senescence-associated β-galactosidase activity and expression of $p16^{INK4A}$ [14].

Because we did not observe any senescent cells in our FBS cultures, we next investigated whether the cultures instead contain quiescent populations. Quiescent cells (G0) express low levels of cyclins [10]. We found that cyclin D1 levels were comparable in FBS and hPL cultures, suggesting that ASCs FBS are in G1 rather than in G0. This implies that ASCs FBS contain slowly proliferating rather than quiescent subpopulations, which is also supported by fact that ASCs FBS proliferate during serial passaging. Alternatively, both of these reversible cell states are present in FBS cultures.

Cyclin D is a major link between mitogenic signalling and the cell cycle machinery [7], and therefore we expected lower levels of cyclin D1 in ASCs FBS. Because we found that cyclin E1 was lower in FBS compared with hPL, our results indicate that cyclin E1 is the rate-limiting cyclin decreasing the rate at which ASCs FBS progress to S phase. This is supported by our cell cycle analysis showing that the G0/G1 phases for FBS were greater than for hPL. Cyclin E has been shown to be essential for G1/S transition [7,8], and its transcription might be dependent on mitogenic signaling [8,33]. However, the lower levels of cyclin E1 may not be the only cause of lower proliferation rates in FBS because we also showed that p21 is increased in FBS compared with hPL.

p21 is involved in regulation of proliferation rates [34] and is expressed by quiescent and senescent cells [9]. Therefore, the higher p21 levels in FBS are not necessarily a sign of senescent subpopulations. It has been shown that mRNA levels of p21 are significantly increased in ASCs FBS at 25 cPDs and at $P \geq 15$

[15,35], indicating that p21 levels increase with increasing senescence in ASCs. We did not detect an increase in p21 mRNA levels in ASCs expanded until P7, which suggests that expression of p21 in FBS is due to normal regulation of proliferation rates. We also found increased levels of p27 in FBS compared with hPL, although not as pronounced as for p21. This might be due to regulation of p27 expression at protein levels.

The transcription factor HES1 ensures that quiescent cells do not transit into senescence [11]. We found great inter-donor variability in expression levels of HES1, which generally tended to be higher in FBS compared with hPL. This might suggest that subpopulations of ASCs FBS are quiescent, whereas other subpopulations are slowly proliferating. However, a larger ASC donor size is needed to be able to draw conclusions. It is also possible that HES1 expression largely is regulated at protein levels.

Hypoxia tended to increase proliferation rates and expression of cyclins E1, A2 and B1 and tended to decrease expression of p21 and G0/G1 fractions in FBS cultures. Several studies have demonstrated significant effects of hypoxia on the proliferation of ASCs cultured in FBS [3–5]. The beneficial effects of hypoxia possibly include hypoxia-mediated up-regulation of ASC paracrine activity and decreased accumulation of reactive oxygen species, compared with expansion at ambient oxygen levels [2,4,5]. However, the effects of hypoxia on hPL cultures were similar to the effects of hPL at normoxia. This implies that hypoxia does not add to the effect of hPL during ASC expansion with regard to proliferation, cell cycle regulation and expression of proliferation-associated genes. Similar results in BMSCs have been obtained by others [36]. Nevertheless, the effects of hypoxia on the regenerative properties of hPL-expanded ASCs, such as secretion of vascular endothelial growth factor and other growth factors, remains to be determined [4,5].

We did not observe significant effects on ASCs FBS hypoxia shifted to hPL hypoxia. The FBS hypoxia group was skewed toward the FBS hypoxia to hPL hypoxia group, and therefore the groups were closer for all comparisons than FBS and FBS to hPL. This could explain why we did not observe an effect.

Our qPCR data generally showed tendencies, with statistical significance at some passages. This is likely due to the relatively low sample size and high inter-donor variability. Whereas TBP and YWHAZ have been proven stabile in ASCs cultured in FBS with increasing passage and at hypoxia [28,29], their stability in ASCs cultured in hPL remains to be determined. However, because FBS and hPL had opposing effects on expression patterns of p21 and cyclins, we do not expect that altered reference genes contributed to these effects.

The majority of studies of human mesenchymal stromal cell senescence have been performed using BMSCs and, to a lesser extent, ASCs. Here, we have discussed our results in relation to other ASC studies when possible, and if not, we have discussed our results in relation to BMSC studies. However, it is important to note that ASCs and BMSCs differ in their senescence mechanism because BMSCs enter replicative senescence earlier than ASCs [31]. Therefore, the results presented here are potentially only applicable to ASCs, because we did not directly compare them to BMSCs. The presence of senescent cells in a clinical ASC product could compromise efficacy [16,17], and senescent ASCs might acquire a senescence-associated secretory phenotype [37,38], which probably interferes with their regenerative effects [39]. Therefore, a senescence potency assay would contribute to assurance of cell product quality [40]. We have shown that ASCs expanded until P7 do not contain senescent cells regardless of the media supplements FBS and hPL and oxygen tension. If ASCs at later passages are used clinically, we suggest that senescence assessment should include (i) screening of ASCs from different donors for $p16^{INK4A}$ expression using qPCR and comparison with previously screened donors and (ii) analysis of responsiveness toward mitogenic stimuli.

Conclusion

Expansion of ASCs in hPL at both normoxia and hypoxia resulted in enhanced proliferation rates; enhanced expression of cyclins E1, A2 and B1; decreased G0/G1 fractions; and decreased expression of cell cycle inhibitors p21 and p27 compared with FBS. We conclude that hypoxia does not add to the effect of hPL during ASC expansion with regard to proliferation rates, cell cycle regulation and proliferation-associated gene expression. The shift from FBS to hPL enhanced expression of cyclins E1, A2 and B1; decreased expression of p21 and p27; and tended to decrease G0/G1 fractions. These results show that ASCs FBS are reversibly arrested and hence not senescent. We therefore conclude that ASCs expanded until P7 are not senescent regardless of the media supplements FBS and hPL and oxygen tension.

Acknowledgments

The authors thank Sofie Lykke Larsen and Kirstine Joo Andresen for their technical assistance. We are grateful to Andreas Printzlau for supplying the liposuction aspirates and the patients for consenting to participate. This work was supported by Arvid Nilsson Foundation, Aase and Ejnar Danielsen Foundation and the Research Foundation, the Capital Region of Denmark.

Disclosure of interest: The authors have no commercial, proprietary, or financial interest in the products or companies described in this article.

References

[1] Zhu Y, Liu T, Song K, Fan X. Adipose-derived stem cell: a better stem cell than BMSC. Cell Biochem Funct 2008;26:664–75. doi:10.1002/cbf.

[2] Hass R, Kasper C, Böhm S, Jacobs R. Different populations and sources of human mesenchymal stem cells (MSC): a comparison of adult and neonatal tissue-derived MSC. Cell Commun Signal 2011;9:12. doi:10.1186/1478-811X-9-12.

[3] Fotia C, Massa A, Boriani F, Baldini N, Granchi D. Hypoxia enhances proliferation and stemness of human adipose-derived mesenchymal stem cells. Cytotechnology 2015;67:1073–84. doi:10.1007/s10616-014-9731-2.

[4] Hung S-P, Ho JH, Shih Y-R V, Lo T, Lee OK. Hypoxia promotes proliferation and osteogenic differentiation potentials of human mesenchymal stem cells. J Orthop Res 2012;30:260–6. doi:10.1002/jor.21517.

[5] Liu L, Gao J, Yuan Y, Chang Q, Liao Y, Lu F. Hypoxia preconditioned human adipose derived mesenchymal stem cells enhance angiogenic potential via secretion of increased VEGF and bFGF. Cell Biol Int 2013;37:551–60. doi:10.1002/cbin.10097.

[6] Juhl M, Tratwal J, Follin B, Søndergaard RH, Ekblond A, Kastrup J, et al. Comparison of clinical grade human platelet lysates for cultivation of mesenchymal stromal cells from bone marrow and adipose tissue. Scand J Clin Lab Invest 2016;76:93–104. doi:10.3109/00365513.2015.1099723.

[7] Hwang HC, Clurman BE. Cyclin E in normal and neoplastic cell cycles. Oncogene 2005;24:2776–86. doi:10.1038/sj.onc.1208613.

[8] Janbandhu VC, Singh AK, Mukherji A, Kumar V. p65 negatively regulates transcription of the cyclin E gene. J Biol Chem 2010;285:17453–64. doi:10.1074/jbc.M109.058974.

[9] Itahana K, Dimri GP, Hara E, Itahana Y, Zou Y, Desprez P-Y, et al. A role for p53 in maintaining and establishing the quiescence growth arrest in human cells. J Biol Chem 2002;277:18206–14. doi:10.1074/jbc.M201028200.

[10] Rando TACTH. Molecular regulation of stem cell quiescence. Nat Rev Mol Cell Biol 2013;14:329–40. doi:10.1038/nrm3591.

[11] Coller HA, Sang L, Roberts JM. A new description of cellular quiescence. PLoS Biol 2006;4:329–49. doi:10.1371/journal.pbio.0040083.

[12] Serrano M. Shifting senescence into quiescence by turning up p53. Cell Cycle 2010;9:4256–7. doi:10.4161/cc.9.21.13785.

[13] Chen J-H, Ozanne SE, Hales CN. Analysis of expression of growth factor receptors in replicatively and oxidatively senescent human fibroblasts. FEBS Lett 2005;579:6388–94. doi:10.1016/j.febslet.2005.09.102.

[14] Shibata KR, Aoyama T, Shima Y, Fukiage K, Otsuka S, Furu M, et al. Expression of the p16INK4A gene is associated closely with senescence of human mesenchymal stem cells and is potentially silenced by DNA methylation during in vitro expansion. Stem Cells 2007;25:2371–82. doi:10.1634/stemcells.2007-0225.

[15] Mitterberger MC, Lechner S, Mattesich M, Zwerschke W. Adipogenic differentiation is impaired in replicative senescent human subcutaneous adipose-derived stromal/progenitor cells. J Gerontol A Biol Sci Med Sci 2014;69:13–24. doi:10.1093/gerona/glt043.

[16] Sensebé L, Bourin P, Tarte K. Good manufacturing practices production of mesenchymal stem/stromal cells. Hum Gene Ther 2011;22:19–26. doi:10.1089/hum.2010.197.

[17] Bieback K, Hecker A, Schlechter T, Hofmann I, Brousos N, Redmer T, et al. Replicative aging and differentiation potential of human adipose tissue-derived mesenchymal stromal cells expanded in pooled human or fetal bovine serum. Cytotherapy 2012;14:570–83. doi:10.3109/14653249.2011.652809.

[18] Griffiths S, Baraniak PR, Copland IB, Nerem RM, McDevitt TC. Human platelet lysate stimulates high-passage and senescent human multipotent mesenchymal stromal cell growth and rejuvenation in vitro. Cytotherapy 2013;15:1469–83. doi:10.1016/j.jcyt.2013.05.020.

[19] Qayyum AA, Haack-Sørensen M, Mathiasen AB, Jørgensen E, Ekblond A, Kastrup J. Adipose-derived mesenchymal stromal cells for chronic myocardial ischemia (MyStromalCell Trial): study design. Regen Med 2012;7:421–8. doi:10.2217/rme.12.17.

[20] Haack-Sorensen M, Friis T, Mathiasen AB, Jorgensen E, Hansen L, Dickmeiss E, et al. Direct intramyocardial mesenchymal stromal cell injections in patients with severe refractory angina: one-year follow-up. Cell Transplant 2013;22:521–8. doi:10.3727/096368912X636830.

[21] Friis T, Haack-Sørensen M, Mathiasen AB, Ripa RS, Kristoffersen US, Jørgensen E, et al. Mesenchymal stromal cell derived endothelial progenitor treatment in patients with refractory angina. Scand Cardiovasc J 2011;45:161–8. doi:10.3109/14017431.2011.569571.

[22] Mathiasen AB, Qayyum AA, Jørgensen E, Helqvist S, Fischer-Nielsen A, Kofoed KF, et al. Bone marrow-derived mesenchymal stromal cell treatment in patients with severe ischaemic heart failure: a randomized placebo-controlled trial (MSC-HF) trial. Eur Heart J 2015;36:1744–53. doi:10.1093/eurheartj/ehv136.

[23] Dominici M, LeBlanc K, Mueller I, Slaper-Cortenbach I, Marini F, Krause D, et al. Minimal criteria for defining multipotent mesenchymal stromal cells. The International Society for Cellular Therapy position statement. Cytotherapy 2006;8:315–17. doi:10.1080/14653240600855905.

[24] Bourin P, Bunnell BA, Casteilla L, Dominici M, Katz AJ, March KL, et al. Stromal cells from the adipose tissue-derived stromal vascular fraction and culture expanded adipose tissue-derived stromal/stem cells: a joint statement of the International Federation for Adipose Therapeutics and Science (IFATS) and the International So. Cytotherapy 2013;15:641–8. doi:10.1016/j.jcyt.2013.02.006.

[25] Follin B, Tratwal J, Haack-Sørensen M, Elberg JJ, Kastrup J, Ekblond A. Identical effects of VEGF and serum-deprivation on phenotype and function of adipose-derived stromal cells from healthy donors and patients with ischemic heart disease. J Transl Med 2013;11:219. doi:10.1186/1479-5876-11-219.

[26] Zuker M. Mfold web server for nucleic acid folding and hybridization prediction. Nucleic Acids Res 2003;31:3406–15. doi:10.1093/nar/gkg595.

[27] Vallone PM, Butler JM. AutoDimer: a screening tool for primer-dimer and hairpin structures. Biotechniques 2004;37:226–31.

[28] Fink T, Lund P, Pilgaard L, Rasmussen JG, Duroux M, Zachar V. Instability of standard PCR reference genes in adipose-derived stem cells during propagation, differentiation and hypoxic exposure. BMC Mol Biol 2008;9:98. doi:10.1186/1471-2199-9-98.

[29] Tratwal J, Follin B, Ekblond A, Kastrup J, Haack-Sørensen M. Identification of a common reference gene pair for qPCR in human mesenchymal stromal cells from different tissue sources treated with VEGF. BMC Mol Biol 2014;15:11. doi:10.1186/1471-2199-15-11.

[30] Stenderup K, Justesen J, Clausen C, Kassem M. Aging is associated with decreased maximal life span and accelerated senescence of bone marrow stromal cells. Bone 2003;33:919–26. doi:10.1016/j.bone.2003.07.005.

[31] Dmitrieva RI, Minullina IR, Bilibina AA, Tarasova OV, Anisimov SV, Zaritskey AY. Bone marrow- and subcutaneous adipose tissue-derived mesenchymal stem cells: differences and similarities. Cell Cycle 2012;11:377–83. doi:10.4161/cc.11.2.18858.

[32] Al-Khalaf HH, Aboussekhra A. p16(INK4A) positively regulates p21(WAF1) expression by suppressing AUF1-dependent mRNA decay. PLoS ONE 2013;8:doi:10.1371/journal.pone.0070133. e70133.

[33] Siu KT, Rosner MR, Minella AC. An integrated view of cyclin E function and regulation. Cell Cycle 2012;11:57–64. doi:10.4161/cc.11.1.18775.

[34] Overton KW, Spencer SL, Noderer WL, Meyer T, Wang CL. Basal p21 controls population heterogeneity in cycling and quiescent cell cycle states. Proc Natl Acad Sci USA 2014;111:E4386–93. doi:10.1073/pnas.1409797111.

[35] Estrada JC, Torres Y, Benguría A, Dopazo A, Roche E, Carrera-Quintanar L, et al. Human mesenchymal stem cell-replicative senescence and oxidative stress are closely linked to aneuploidy. Cell Death Dis 2013;4:e691. doi:10.1038/cddis.2013.211.

[36] Holzwarth C, Vaegler M, Gieseke F, Pfister SM, Handgretinger R, Kerst G, et al. Low physiologic oxygen tensions reduce proliferation and differentiation of human multipotent mesenchymal stromal cells. BMC Cell Biol 2010;11:11. doi:10.1186/1471-2121-11-11.

[37] Severino V, Alessio N, Farina A, Sandomenico A, Cipollaro M, Peluso G, et al. Insulin-like growth factor binding proteins 4 and 7 released by senescent cells promote premature senescence in mesenchymal stem cells. Cell Death Dis 2013;4:e911. doi:10.1038/cddis.2013.445.

[38] Sepúlveda J, Tomé M. Cell senescence abrogates the therapeutic potential of human mesenchymal stem cells in the lethal endotoxemia model. Stem Cells 2014;32:1865–77.

[39] Caplan AI, Dennis JE. Mesenchymal stem cells as trophic mediators. J Cell Biochem 2006;98:1076–84. doi:10.1002/jcb.20886.

[40] Galipeau J, Krampera M, Barrett J, Dazzi F, Deans RJ, DeBruijn J, et al. International society for cellular therapy perspective on immune functional assays for mesenchymal stromal cells as potency release criterion for advanced phase clinical trials. Cytotherapy 2016;18:151–9. doi:10.1016/j.jcyt.2015.11.008.

Appendix: Supplementary material

Supplementary data to this article can be found online at doi:10.1016/j.jcyt.2016.09.006